MIPS Campaign A1

MIPS Team

September 10, 2003

Abstract

MIPS Campaign A1 was conducted between 0115 and 0300 UTC September 2. All sequences ran as expected, and good data were obtained. The status of the instrument so far as it can be determined this early in the SIRTF mission is consistent with its state in ground testing prior to launch, except that one readout on the 70 micron array that returned useful data on the ground is no longer doing so. Readout 3 is not operating correctly on the 160μm array, and the contingency plan for this problem needs to be implemented.

1. Campaign Goals

Campaign A was the initial opportunity for turning on the Combined Electronics as well as the MIPS instrument. The goals were to verify the overall health of the electronics and to conduct aliveness testing on the cold MIPS instrument functions. It was expected that all the detector arrays would be hard saturated at the background levels so early in the mission, so their health would have to be judged in a preliminary way based on the groundbased aliveness test (e.g., no meaningful noise limits can be determined). Also, verify the 24μm RAW and SUR observation modes. Additional goals were: verify scan mirror motions, stim flashes, and basic commanding by running a photometry AOT; check coadding and prove that the system can handle collecting data in the most demanding possible observing mode; verify thermal control of the 24μm array; and perform thermal anneals on all three arrays and show that the temperature profiles are as expected.

2. Task Outline

The sequence of activities in Campaign A1 is summarized in the following table.

Task	Description
MIPS-010 MIPS Campaign Start-up Activities,	Turn on power to the combined electronics Transition from OFF to MIPS_OBSERVE
MIPS-015 CE State Validation and Functional Tests	1) Perform thermal anneals on all three arrays, using diagnostic data collection mode to monitor temperatures (see MIPS Functional Test) 2) Switch to the B-side Si heater and command it to 5.2K. 3) Perform the mips_mobs_phot state transition 4) Point the scan mirror to the 24μm dark position, and take a set of 10 4s DCEs in RAW mode. Change the Ge Vrst values to place negative bias on the arrays, and collect 10 3s DCEs in SUR mode. Return the Vrst

	voltages to their nominal values. (See the MIPS aliveness test for appropriate Vrst settings for putting negative bias on the arrays.) 5) Run a MIPS Worst Case Processor Load Test by sending the command MIPS_SmplUpRamp_C3F61N5_MIPS (coadd=8, framecount=61, number of DCEs=5, SUR mode, runtime = 5 minutes) 6) Perform the mips_backto_mobs state transition 7) Run a 70µm compact source photometry AOT
MIPS-950 Scattered Light Background Monitor	Acquire dark measurements for 24, 70, and 160 µm using the standard dark IERs.
MIPS-090 MIPS Campaign Shutdown Activities	Transition from MIPS_OBSERVE to OPERATE

3. Results

3.1. Performance of Combined Electronics

There were no significant anomalies in the performance of the electronics (the tests were run on CE1). All sequences ran flawlessly. Upon turnon, a small number of limits were triggered. With two exceptions, they were associated with turnon transients and were of no significance to the operation of the electronics. The exceptions were the currents to the 70 micron array, which were extremely low. Low currents are expected when the array is saturated (and drives the readout amplifiers to a configuration with small current draw). The observed currents were lower than had been seen in ground test, but were the same for both sides of the array (indicating that there were no failures, since the sides are completely independent and a failure that occurred in both identically would be very unlikely). We decided that these values were because the backgrounds were higher than had been the case for any of the ground tests, and this hypothesis was confirmed when the array data showed correct operation.

The CE housekeeping data were nominal. The temperatures were well within the permitted operating range. Approximately 1200 exposures were acquired, with about 50 seconds in silicon RAW mode. In addition, there was a CPU stress test. All of these activities were successful with no indications of issues in passing the data to the spacecraft or to the ground.

We ran a Photometry AOT successfully, indicating that all the communications with the spacecraft are in place.

3.2. Performance of Cold Instrument

3.2.1 24 Micron Array

The 24 micron array was in hard saturation, even in the first differences (0.5 seconds integration). We were able to catch the array pre-saturation in the sample just after reset (see Figure 1). The data indicate that it is fully operative, with no major changes from the state on the ground. The zero point was as expected. The array heater put its temperature at 5.2K. There were a number of alarms associated with the heater operation.

3.2.2 70 Micron Array

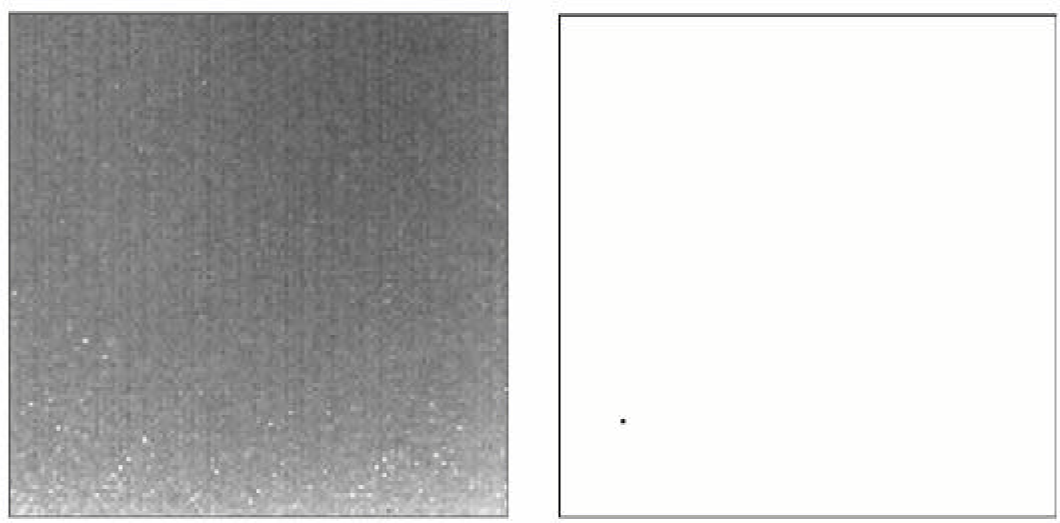

Figure 1. The left frame is the sample immediately after a reset, the right one is the next frame. The left frame indicates the array was caught just before saturation, while it is fully saturated to the right. We conclude that the array is probably fully operational.

This array was also in hard saturation. The data indicated that it was operative, with one major change from the state on the ground. The readout with an output cable short to CTA chassis ground still has this short. It has a nominal value of about 40 Kohms, similar to the value after the acoustic test at Lockheed. The instrument testing indicated that this readout is unlikely to be corrupted by excess noise with this value for the short, but that its output will be pulled down modestly. We therefore expect a small degradation in performance, but that the data obtained with these 32 pixels will be fully usable. We will also not have to apply the mitigation procedures we had developed in case the short was less than 2 Kohms.

Unfortunately, we found that readout 4,4 was inoperative, representing a new failure. We show the layout of the array in Figure 2. Readout 4,4 is to one edge and next to the center line (see Figure 3). We have carried out a detailed analysis of this failure, attached as an appendix.

A review of the telemetry shows that the two sides of the 70µm array have identical power draw to observations on the ground to within 1%. The I_{dduc} values were around 14µA, lower than we have seen before, but probably only because of the very high background from the telescope. V_{reset}, V_{bias}, V_{offset}, and V_{Iload} were all close to the values seen on the ground.

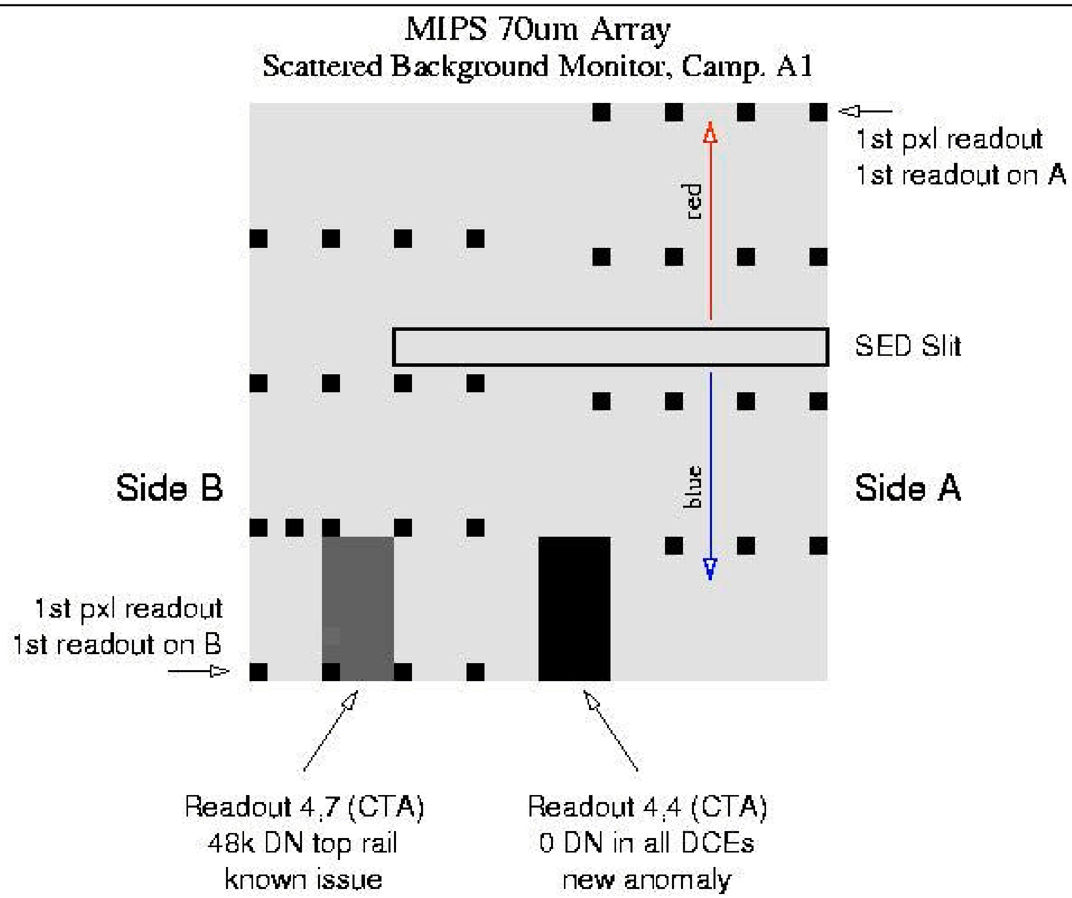

Figure 2. Layout of the 70µm array. We indicate the read order for the pixels, the position of the SED slit, and the locations of the dead readout and of the readout with the short to chassis ground.

We were able to verify that parts of the array were integrating. The array reset is global (all pixels simultaneously) and it is then read out sequentially starting as indicated in Figure 2. Thus, the shortest times between reset and the first read are at the upper right for readouts on Side A and at the lower left on Side B of the array. Figure 3 shows the comparison of array images with the scan mirror in the two "dark" positions. Saturated is white (and the scaling does not show the two offset readouts). It can be seen that the background is lower (more out-of-saturation pixels) in the 160µm dark position, which is also the SED position. Non-saturated signals are seen from all readouts except 4,4 in that position. In addition, the fact that the backgrounds change when the scan mirror is commanded to move indicates that it is in fact moving. The scan mirror telemetry is also normal, indicating that it is operating correctly. In addition, the images show that the pixel orientation is as expected.

More subtle indications of correct instrument operation from Figure 3 are that the slit is to the right, with the blanked off region occupying 7-8 pixels to the left (they are noticeably less saturated), and that in the region under the slit, there is stronger illumination toward the bottom. The bottom region is where the “blue” = 50µm light should fall, and given the high temperature of the telescope, should be brighter than the top “red” = 100µm zone.

3.2.3 160 Micron Array

This array was also in hard saturation. The data indicated that it was operative, except on readout 3. The behavior of readout 3 is similar to that observed in the thermo/vac test. It will be necessary for the SSC to implement the mitigation plan that was developed as a result of the failure of the cables associated with this readout. This plan primarily calls for modification of the AOR to put the observations in an “optimum” position for

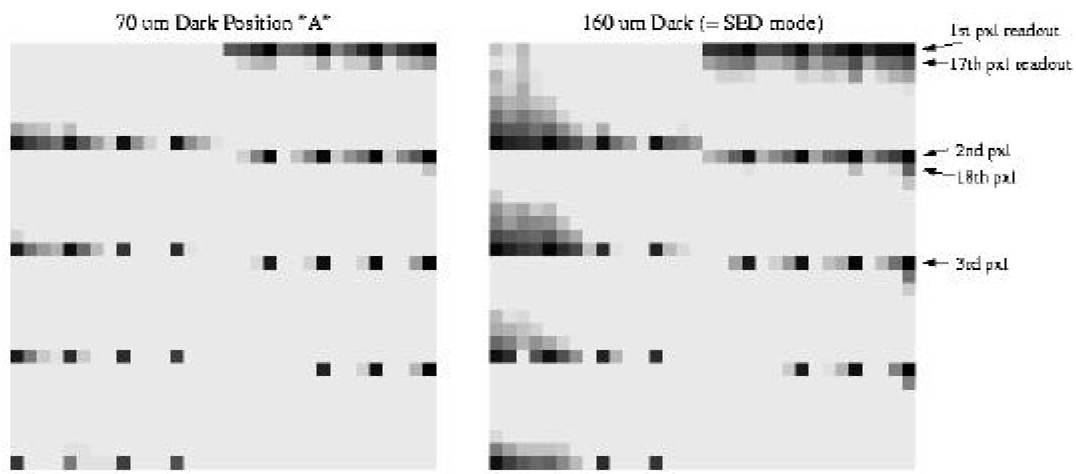

Figure 3. Comparison of images in the two “dark” positions.

photometry, plus adjustment of stim levels. For scan map, many programs will suffer a degradation in redundant coverage of the sky that will have to be addressed by additional passes or similar modifications.

Readout 5 shows a very small offset, similar to one that was seen in the first warm soak in thermo/vac but which was absent in the second warm soak. We believe that this offset can be accommodated within the dynamic range of the electronics, and that valid data will be obtained with these pixels. This assumption requires that the behavior of the readout be stable, which has not yet been tested with the detectors operating at superfluid temperatures.

A more detailed report on the scattered light monitoring by James Muzerolle, John Stansberry, and Erick Young is available on the MIPS IOC website.

3.3. Other Instrument Functions

3.3.1. Anneals

All array anneal heaters were operated successfully. For the silicon array, we expected the anneal enable signal to go to disable when the anneal was turned off, but it did not – we are investigating whether this is the correct behavior.

3.3.2. Stimulators

The stimulator circuits operated correctly. We have no direct feedback to show that the stimulators themselves operated; we will have to wait for the background to drop so we can see if the stimulator outputs are detected.

3.3.3. Scan Mirror

The scan mirror was commanded to move, and from the behavior of its drive current we conclude that it did so correctly. Since it is a servo mechanism, failure to move to the commanded position would have left the servo out of balance, resulting in a progressive increase in drive current until a limit was tripped (causing the CE to suspend).

Additional evidence for the correct operation of the scan mirror was discussed in Section 3.2.2.

3.3.4 Telemetry

The telemetry has been reviewed in great detail to identify any items that depart from expectations. A few issues have already been identified. Additional ones are:

- Temperature readings were strange in various ways for three thermometers. We need to see if the correct calibration curves are loaded for them.
- A known error in the CalibCyclCmd appeared. A correction was already scheduled for later in IOC.
- The FIFO timeout counter triggered a number of times when it was not expected. This counter indicates when data are coming into the FIFO so slowly that a transfer needs to be initiated without waiting for the FIFO to get more than 50% full.

A detailed analysis of the telemetry by Doug Kelly is available on the MIPS IOC website.

3.3.5 Alarms

A large number of alarms appeared at time 03-245T01:21:47.230, coinciding with the OFF_BOOT state transition. There is a short time during this state transition when the CEState is indeterminate, the telemetry values are invalid, and a large number of false red alarms appears. The same is true during the BOOT_OPR transition at 03-245T01:26:11.230, the MIPS_OPR_MRDY transition at 03/245-01:32:55.328, and the MIPS_MRDY_OPR state transition at 03/245-02:57:19.289. Information on when each of the telemetry values is valid should be incorporated into the alarm-checking software to reduce the number of false alarms.

Four alarms were triggered by very low values for the 70μm array I_{dduc} current, which was low because the huge background had driven the readout into hard saturation and pinched off much of the amplifier current. Correct operation of the array is indicated in other ways, see Section 3.2.2. These alarms should cease to be an issue once the telescope is cold. The corresponding alarms for the 160µm array only triggered during telemetry transients.

The U AnCSM_Curr was found to have an incorrect low limit.

A number of alarms were associated with temperature sensors.

A detailed analysis of the alarms by Tom Glenn and Doug Kelly is available on the MIPS IOC website.

4. Conclusions and Consequences

Overall, MIPS is in good health so far as can be told from the results of Campaign A. A number of items need "tuning up" as indicated from the telemetry and alarms, but none of them represent any issue for further operation of the Combined Electronics or the cold instrument. The instrument seems to be very close to its state in prelaunch testing, with the exception of the loss of signal from one readout in the 70µm array. Readout 3 on the 160µm array is not operating correctly, as seen on the ground, and we should start implementing the contingency plans for this problem.

MIPS 70 Micron Array Readout (Channel 2) Anomaly
ISA Z81711

Erick Young, George Rieke, Jerry Heim, John Stansberry, Doug Kelly, and Tom Glenn

September 9, 2003

1. Summary

In reviewing the data from MIPS Campaign A1, it was found that one readout of the 70 μm array was at the negative rail. The other readout outputs were at the positive rail due to saturation on the strong signals from the telescope. Therefore, there is an anomaly affecting the readout (number 4,4).

We have reviewed prelaunch test data and found that the readout was operating correctly then. We have also gone back to data independently of the MIPL processing and found that the readout 4,4 data were railed negative there. We therefore conclude that the issue is new and is in the flight hardware.

In Campaign B, we found that readout 4,4 was operating correctly – the anomaly had apparently been corrected. Before this anomaly is fully resolved, we will have to track the behavior of the array for a number of additional campaigns. However, the situation is well enough defined for a report on possible causes.

2. Anomaly Description

A greyscale representation of the output of the 70 μm array as it was throughout Campaign A1 is shown in Figure 1. Figure 2 shows the array output levels. Readout 4,4 is at zero for the duration of the test, and was not seen to deviate from this reading throughout Campaign A1. All the other readouts were saturated positive by the very high background level from the relatively warm telescope, except for readout 4,7. That readout was known prior to launch to have a short on its output to chassis ground through a resistance of approximately 40 kΩ. The resultant loading of the signal puts the saturation level below the nominal rail of the system. The data in Figure 2 indicate that the value of the short has not changed substantially between ground test and the on-orbit data.

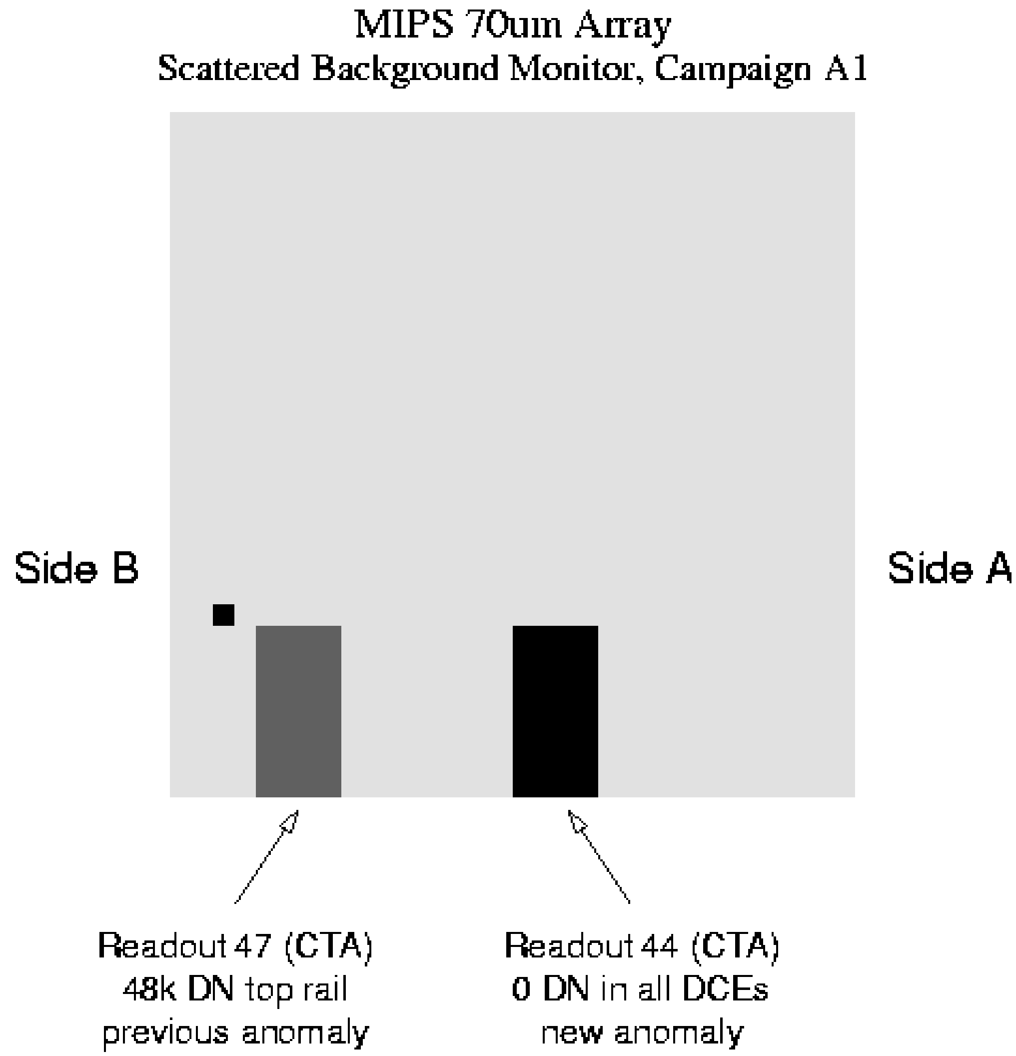

Figure 1. 70mm Array Output. Readout coordinates start in the upper right corner. Readout 4,4 is driven hard to the negative rail. Readout 7,4 has a short to chassis ground similar to that observed previously. There is a bad pixel on readout 8,3.

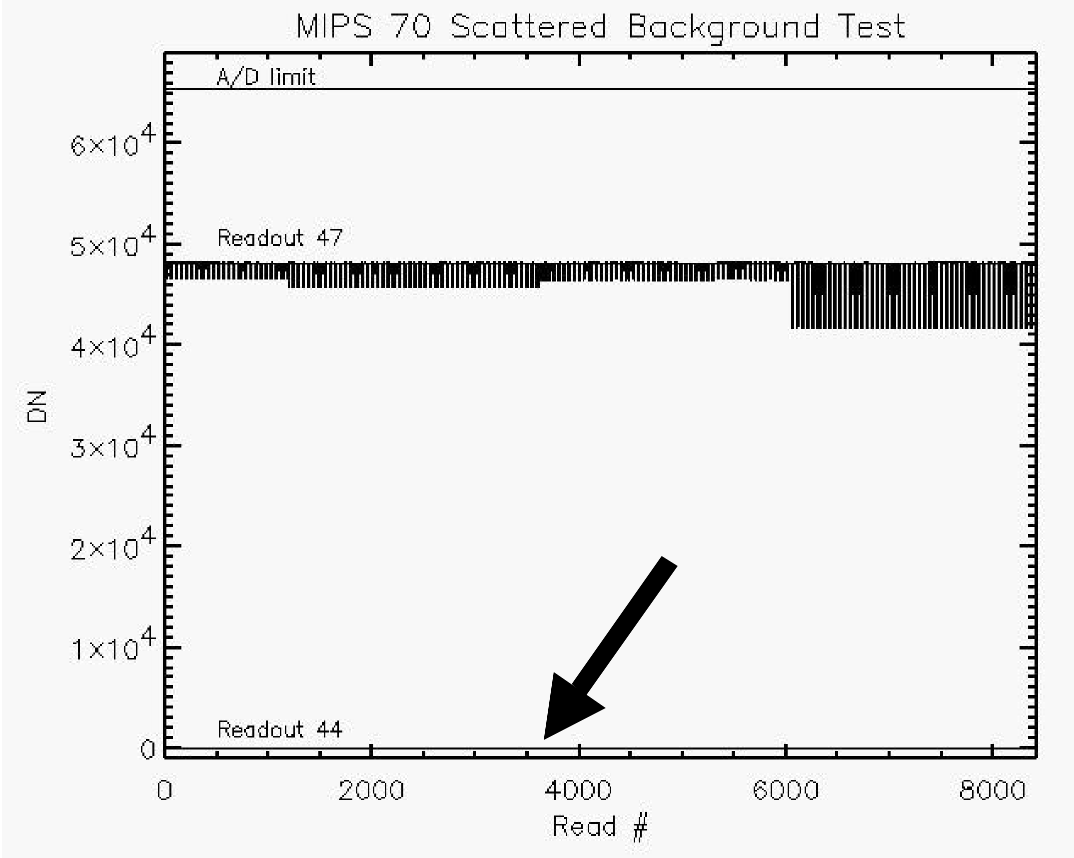

Figure 2. 70mm Array Outputs. 30 of the outputs were at the A/D limit, indicating full saturation. Readout 4,7 is also indicating saturation, but its output is dragged down by the partial short to CTA chassis ground. It also shows vestigial integration ramps that are off scale for the other readouts. Readout 4,4 (indicated by the arrow) is at zero and remained there throughout the test.

3. Failure Analysis

Figure 3 below shows the overall layout of the MIPS electronics. The cabling between array and warm electronics is shown in Figure 4 (reversed from right to left compared with Figure 1). Failures can arise in: 1.) the array; 2.) the cabling between warm electronics and array; or 3.) the warm electronics. The correct behavior of the remaining readouts in the array, and the restoration of correct behavior on readout 4,4 during Campaign B, both indicate that there is no problem on the digital side of the circuit, nor in the computer program that handles the data.

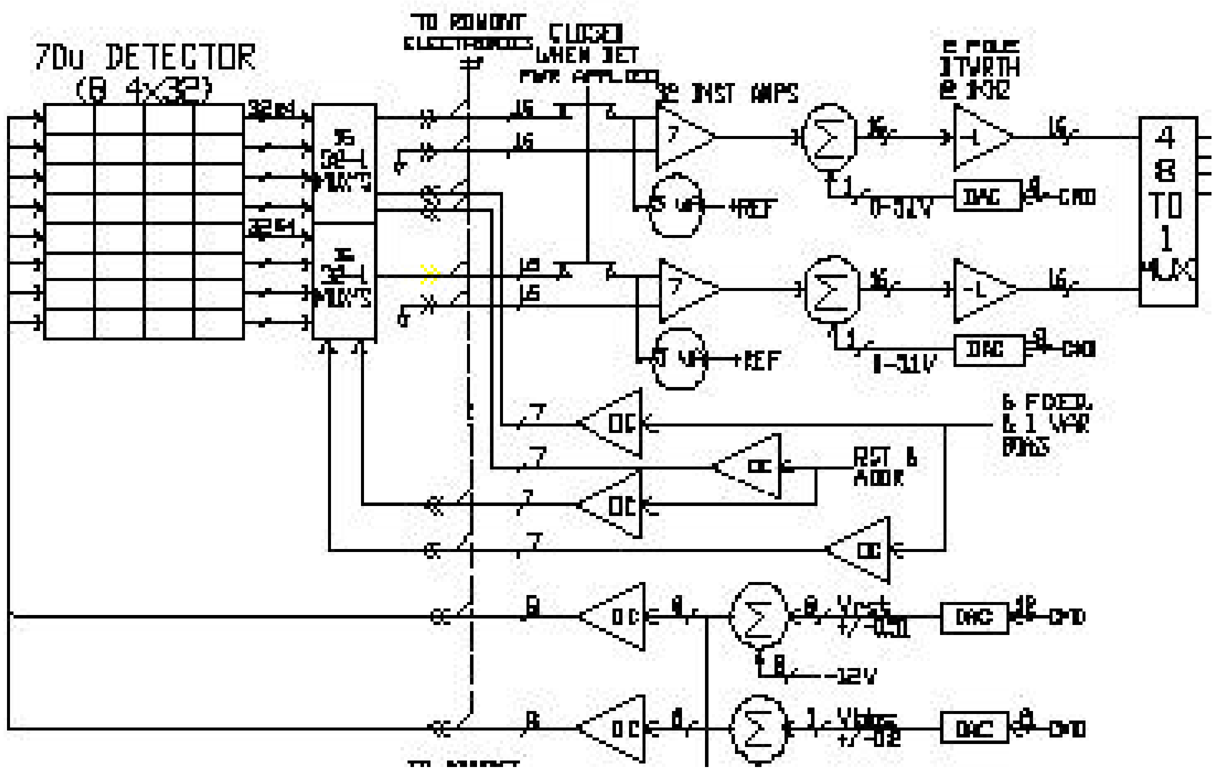

Figure 3. Overall layout of the electronics. The transition from cold to warm is the dashed vertical line. Signals from 4x8 pixel sections of the array are brought to a 32-channel readout and then through the cryostat wiring to the warm electronics. There, they are received by a differential amplifier, pass through an offsetting amplifier and filter, and are delivered to the MUX and A/D.

3.1 Array Failures

The possibilities we have identified for a failure within the array are either that the readout itself has failed, or that a wire bond bringing a power line to the readout or carrying the signal to the output connector has broken (see Figure 5). A careful review of the telemetry indicates no asymmetry between sides A and B of the array in current draw, and no significant differences from ground readings except for those resulting from the very high background. In general, failure of the readout or of a power line would be reflected in a change in current draw. We conclude that a failure within the array other than in the output wirebonds is unlikely.

3.2 Cable Failures

External to the array, the failure could result from a break in the readout wire in the instrument cabling or connector, in the CTA ribbon cabling or connectors, in the spacecraft cabling from the junction box to the electronics, or in the junction box.

In the Combined Electronics box, for each of the 32 readouts of the 70μm FPA there is a 5 micro-amp current source in the warm electronics that is used to bias the source follower output amplifier in the FPA. This current source is also connected to the instrumentation amplifier in the combined electronics. If the connection between the current source and the output amplifier is broken, the current source would go to its positive rail voltage (about +7V). The instrumentation amplifier and the low-pass filter that follows have gains of –7. Thus, if the connection were broken, the output of the low-pass filter would go to the negative rail. With the filter output at the negative rail, the ADC would produce all zeros. This is exactly what we are seeing.

A review of the positions of the wires involved indicates none of them are at the end of a connector, making it unlikely that the failure arises through a partially seated connector. Nonetheless, a workmanship issue in attaching to a connector pin or something similar remains a possibility. Issues of this latter type have already been discovered in the cryogenic ribbon cables, during ground testing.

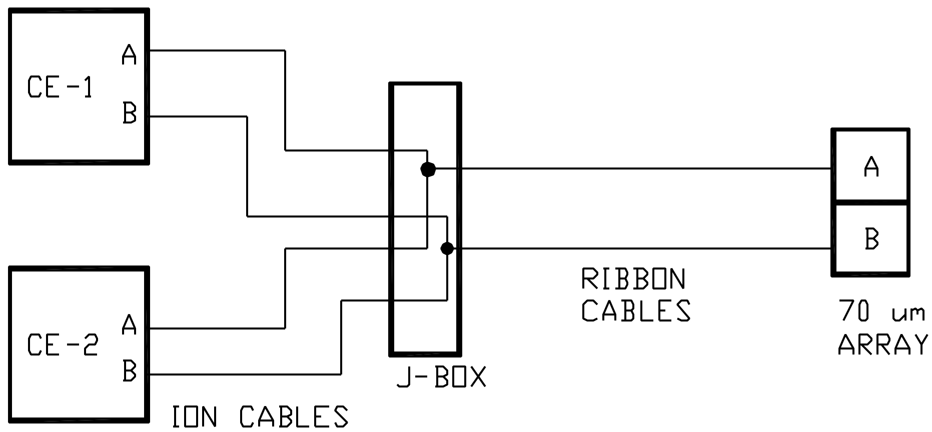

Figure 4. Cabling diagram between detectors and warm electronics.

3.3 Warm Electronics Failures

Figure 6 shows the receiver differential amplifiers in the warm electronics boxes. The decoupling relays allow the signals to be isolated to the box in use. Just as with an open signal cable, the differential amplifier would drive to the rail if the decoupling relay or electronics box connectors have failed open. In addition, there could be a failure in the differential amplifier itself. We could also end up at the rail with failures in any of the analog chain components downstream of it, up to the multiplexer. Finally, there are possible generic electronics failures such as in the motherboard in the electronics, in solder joints, etc.

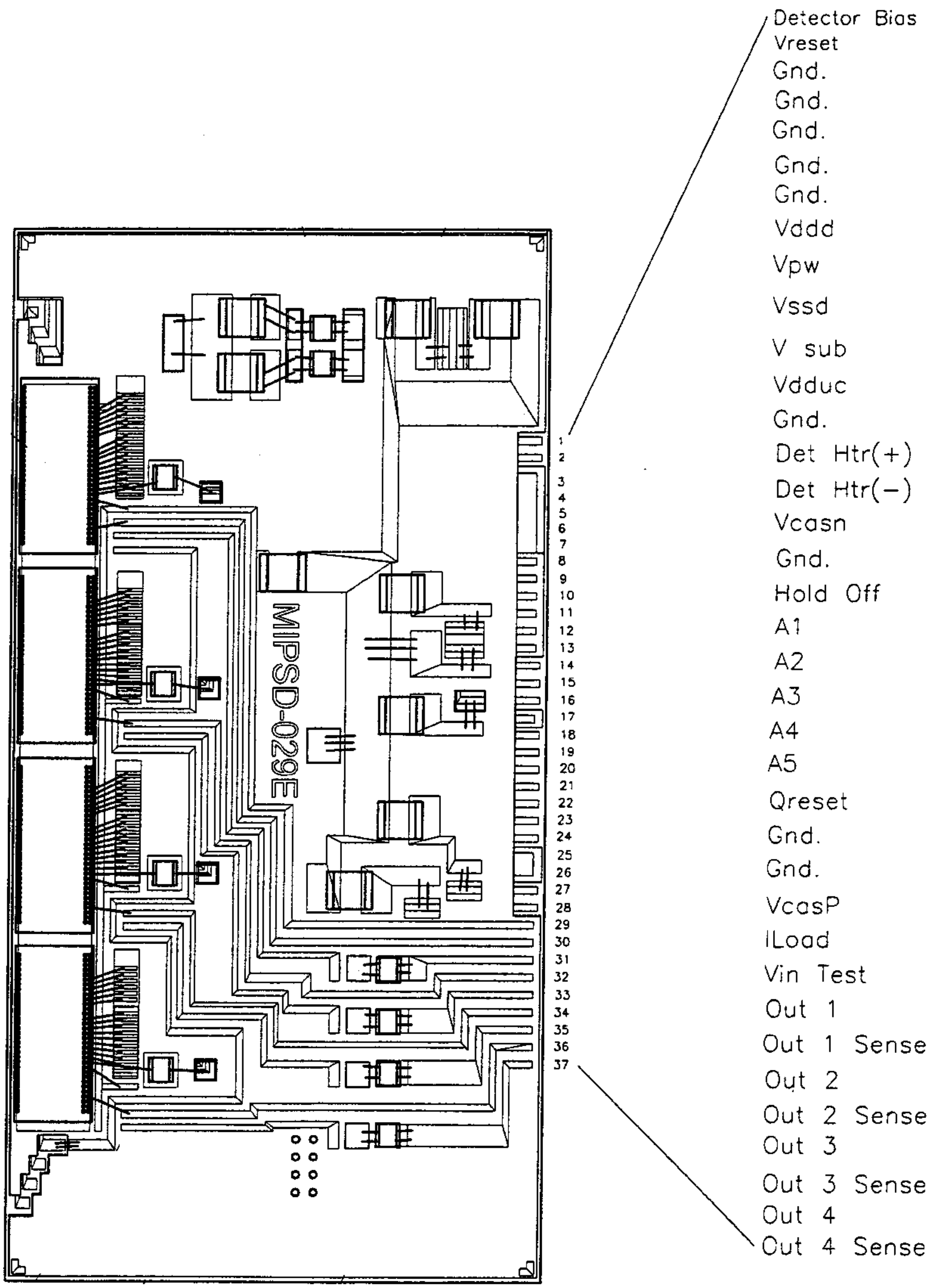

Figure 5. Ceramic multilayer board carrying four readouts for the 70 micron array.

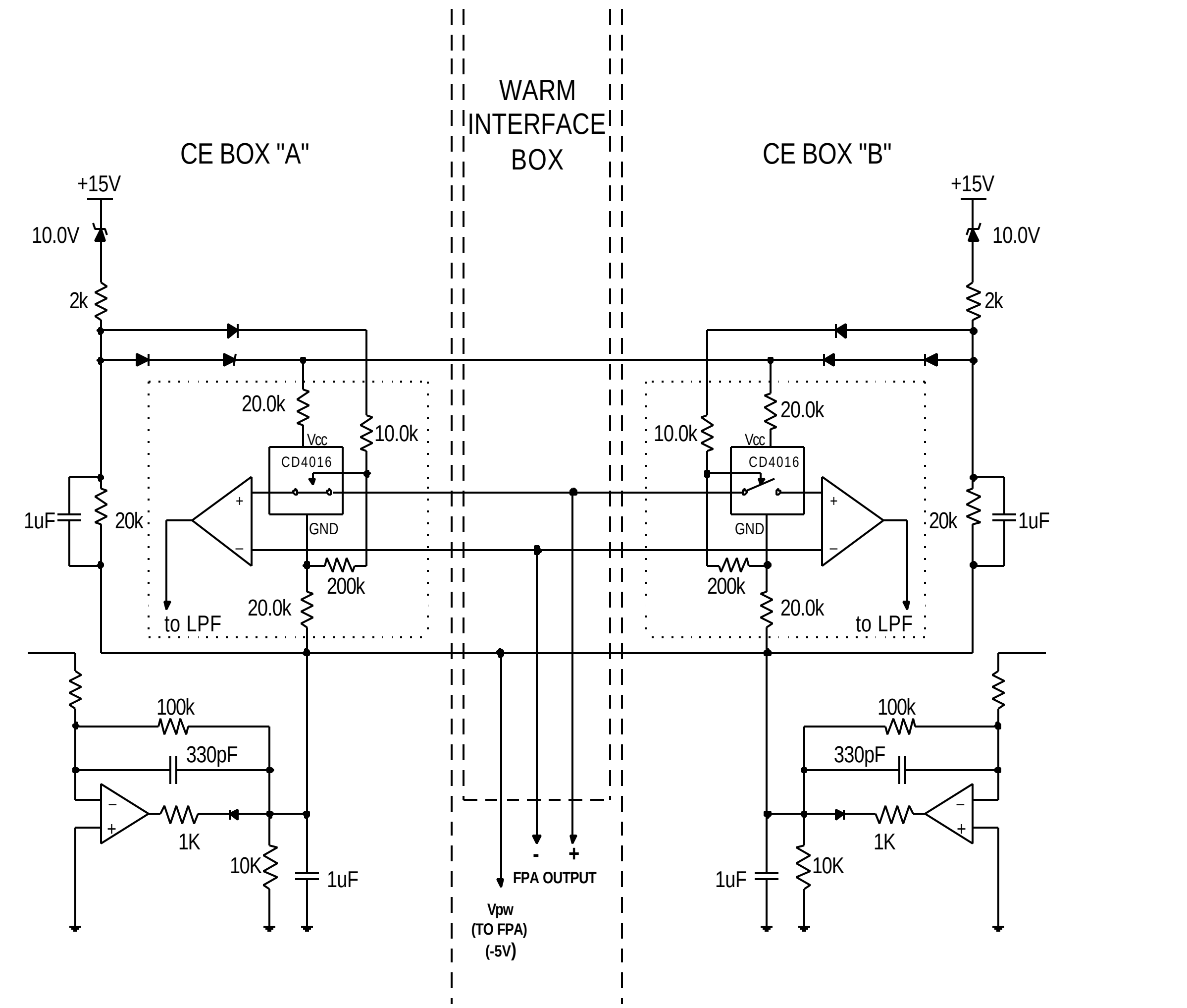

Figure 6. Differential amplifier receiver circuits for the two warm electronics boxes.

3.4 Eliminated Failure Mechanisms

We have also eliminated a number of possible failure mechanisms:

- As shown in Figure 5, the input signals to the readout are common to three other readouts, with the necessary circuitry embedded in the multilayer ceramic board carrying the readouts. Therefore, cable failures affecting input signals are not a credible cause for the anomaly.
- An output short to chassis would not drive the output to the negative rail – the observed fault would require a short to a positive supply, which seems contrived.
- An open sense line for readout (4,4) would not produce the result because the electronics includes a resistor on the sense line to ground to guard against this possibility.

3.5 Failure Propagation

Reviewing these possible causes, and non-causes, there appears to be no danger of the failure propagating in any avoidable manner if we continue to operate the array, or operate it on the other combined electronics unit. Fundamentally, the likely failure mechanisms are isolated in their effects to the analog data chain associated with readout 4,4. The data line with the anomalous behavior carries only a low-power analog signal.

4. Analysis

With the possible causes of the failure isolated, we can sort through them making use of the additional information that the failure disappeared in Campaign B. This change is presumably associated with some change in circumstances.

One candidate failure mechanism is a latch condition that was reset by turning the Combined Electronics off at the end of Campaign A1 and back on for Campaign B. However, we have never seen such a condition during ground test. Such testing was conducted with the electronics close to its current operating temperature, and during Thermo/Vac, at extremes of temperature that bracketed the current on-orbit temperature. It therefore is unlikely that this explanation holds.

Failures within the array are similarly unlikely. In this case, the only change in environment is a slight cooling as the cryostat bath pumps down on orbit. However, the temperature of operation for both Campaigns A1 and B was within the range included in our groundbased testing. In addition, the temperature change between the campaigns is too small for a fault due to the launch conditions to change state.

The cryogenic cables have experienced significant changes in temperature between the two campaigns, due to the cooling of the telescope and various shields. Most of the thermometers associated with the telescope show a change of about 40K, from about 120K to about 80K. The behavior of the SIRTF cryogenic ribbon cables has been studied as described in Ball Aerospace SER S20447 – I&T (June 17, 2002). Of three flight spare cables, one showed a bad wire. The behavior was not reproducible from one cryogenic cycle to the next, but often problems appeared near temperatures of 100 to 150K. On some cycles, the conductor never failed completely down to < 100K. In tests of a second cable, known to have a bad attachment to a connector pin and removed from the flight hardware for that reason, intermittent behavior was observed during one thermal cycle but no hard failure occurred. From these tests, it does appear plausible that the behavior we have seen on readout 4,4 is associated with a bad conductor carrying its signal from the instrument to the junction box.

We therefore propose that the explanation for the anomaly on the readout 4,4 output is an intermittent failure on its output cable. Because we do not have data on the behavior of the cable at lower temperatures than achieved for Campaign B, it is not possible to project whether the problem is “fixed” as seen in that campaign, or whether the cable will open again later in the mission.

Given the uncertainty in the future state of this cable, we recommend that contingency planning continue on modification of the observing strategies with the instrument in case the readout output is lost.